Volume 16, Issue 3, 162413 (1-14)

Iranian Journal of Earth Science (IJES)

https://dx.doi.org/10.57647/j.ijes.2024.1603.13

Geochemical (Ti–Mg) characteristics of the Proterozoic mafic metavolcanic rocks of Raialo Group of Alwar sub-basin, North Delhi Fold Belt, NW India

Mukesh Bairwa*, Manoj Pandit

Department of Geology, University of Rajasthan, Jaipur, India.

*Corresponding author: profmk.bairwa@gmail.com

Original Research

Received:
5 June 2023
Revised:
9 Aug 2023
Accepted:
17 Sep 2023
Published online:
15 July 2024

Abstract:

The Mesoproterozoic North Delhi Fold Belt (NDFB) represents the northeastern limit of the Aravalli–Delhi Fold Belt in the NW Indian craton. The mafic metavolcanic rocks from the Tehla–Pandupol region of the Raialo Group were investigated from the southern part of the Alwar sub-basin of NDFB. In this preliminary study, we present broad geochemical groupings of these rocks and attempt to decipher their petrogenesis and tectonic setting. The mafic metavolcanic rocks are gray to greenish gray, compact to foliated, and commonly occur as ground-level exposures, occasional hillocks, and along the lower flanks of quartzite ridges. Their mineralogical and textural attributes suggest variable degrees of alteration and greenschist to lower amphibolite facies metamorphism. Geochemically, these rocks can be subdivided into three broad types; low Ti –high Mg, moderate Ti –moderate Mg, and high Ti –low Mg groups. Trace element characteristics of low- and medium- Ti groups (the early phases) show a notable crustal input while the most evolved, high- Ti group seems to be generally unaffected by crustal contamination. Systematic variation in geochemical characteristics during progressive differentiation and REE characteristics define a genetic relationship between low and moderate Ti groups while high- Ti represents a distinct group, unrelated to the rest.

Keywords: Mafic metavolcanic rocks; Geochemistry; Ti–Mg characteristics; Raialo group; North Delhi Fold Belt; Nw India

1. Introduction

Basic rocks are the most suitable candidates for evaluating the upper mantle composition and mantle evolution through geological times, on account of their derivation exclusively from the melting of a mantle source (Wilson, 1989). Their geochemical characteristics not only provide an insight into the mantle composition but also help in understanding the crust-mantle interaction as the high-temperature basic magmas would interact with and assimilate the crustal rocks during the passage through the crust, and eventual extrusion/emplacement. Therefore, basic magmatic rocks have been extensively studied and several geochemical discrimination schemes have been proposed for their source evaluation and tectonic setting (Pearce and Norry, 1979; Pearce and Peate, 1995; Dilek and Furnes, 2011; Verma and Agrawal, 2011; Niu, 2018; Dabiri et al., 2018-a; Pearce et al., 2021; Nazari et al., 2023; Ousta et al., 2024) and references therein. In the Indian context, the Cretaceous – Paleogene age Deccan basalts have attracted global attention on account of their association with the Reunion Plume, vast expanse (∼500,000 km^2 area), well-exposed sections and unaltered nature (Subbarao and Hooper, 1988; Natali et al., 2017) and references therein. These rocks have provided useful information about the late Mesozoic mantle, however, not much is known about the Precambrian mantle of subcontinental India because the older mafic rocks have either been eroded or completely altered and transformed in this region (Ramakrishan and Vaidyanadhan, 2008) as the mafic rocks are susceptible to erosion and alteration. Mafic volcanic rocks are an essential component of the rift-sedimentary sequences and are known from various Precambrian rift basins

of India (Ramakrishan and Vaidyanadhan, 2008). Geochemical characteristics of mafic volcanic rocks of the Dharwar Craton greenstone belts in southern India have provided an insight into the nature of the south Indian Precambrian mantle (Drury, 1982, 1983). Mafic volcanic rocks are also known from the Aravalli basin in northwestern India where they occur interlayered with metasedimentary rocks (Sinha-Roy et al., 1998; Roy and Jakhar, 2002). Their Sm-Nd data could not yield any meaningful ages but reported Nd model ages range from 2600 to 2300 Ma (Ahmad et al., 2008) and references therein, while, some studies have provided geochemical details of these rocks (Abu-Hamatteh et al., 1994; Abu-Hamatteh, 2002). Although basic volcanic rocks have been reported from the Meso- Neoproterozoic Delhi Supergroup (Gupta et al., 1980), not much is known about their geochemistry, probably on account of isolated and scanty exposures. In the northern sector of the Delhi Fold Belt, mafic volcanic rocks have been reported from the Bayana – Lalsot and Alwar sub-basins (Gupta et al., 1997; Sinha-Roy et al., 1998; Roy and Jakhar, 2002). The mafic volcanic rocks in the southern part of the Alwar sub-basin (Proterozoic Delhi Supergroup) represent an important unit of the Raialo Group, which is the lowermost stratigraphic unit of the Delhi Supergroup. Although general geochemical characterization of basic volcanic rocks from some parts of the Alwar and Bayana – Lalsot sub-basins in this domain has been provided by Raza et al. (2001) and Raza et al. (2007) and Raza et al. (2014), their counterparts from the southern part of the Alwar sub-basin have not received much geochemical attention. We have studied the Raialo Group basic metavolcanic rocks from the Tehla – Pandupol area where they show the best development (Fig. 1 b). In this paper, we provide an overview of geochemical characteristics of these mafic volcanic rocks (subsequently metamorphosed) and discuss (i) their Ti and Mg characteristics, (ii) the geochemical discrimination and identification of three geochemically distinct groups in the area, and (iii) have attempted to evaluate their petrogenesis and mutual relationships. This contribution presents the preliminary geochemical characteristics of mafic meta-volcanic rocks of the southern part of the Alwar sub-basin for the first time. Detailed geochemical and isotopic analyses of the mafic meta-volcanic rocks are underway and will be included in a follow-up publication.

2. Geological setting

2.1 Geological overview

The Aravalli Delhi Mobile Belt (ADMB) forms the most prominent Proterozoic supracrustal sequence in the northwestern part of the peninsular Indian shield (Fig. 1 a). The Archean basement in this region comprises TTG gneisses 3.3 Ga – (Wiedenbeck et al., 1996), metasediments, and granites 2.5 Ga – (D'Souza et al., 2020), collectively named Banded Gneissic Complex by earlier workers BGC – (Gupta, 1934; Heron, 1953). The basement rocks of NW India were regrouped by Gupta et al. (1980) who coined the term Bhilwara Supergroup which also includes a Paleoproterozoic component, and further subdivided the basement into Hindoli Group, Mangalwar Complex, and Sandmata Complex. The basement is overlain by two volcano-sedimentary sequences, an older Aravalli Supergroup (Palaeo- to Mesoproterozoic) and a younger Delhi Supergroup (Mesoproterozoic) (Heron, 1953; Sinha-Roy et al., 1998; Roy and Jakhar, 2002). The southern domain of the ADMB mainly constitutes the Udaipur- Jharol Belt of the Aravalli Supergroup (Roy and Paliwal, 1981) and the Pindwara – Sirohi sector of the Delhi Supergroup (Gupta et al., 1980).

Sinha-Roy (1984) proposed a diachronous sedimentation history for Delhi Supergroup and subdivided it into two distinct geographic domains, viz. an older North Delhi Fold Belt (NDFB) and a younger South Delhi Fold Belt (SDFB). This subdivision, based mainly on the difference in the intrusion ages, was contested by some other workers (Roy and Kataria, 1999; Bose et al., 1996). Singh et al. (2010)

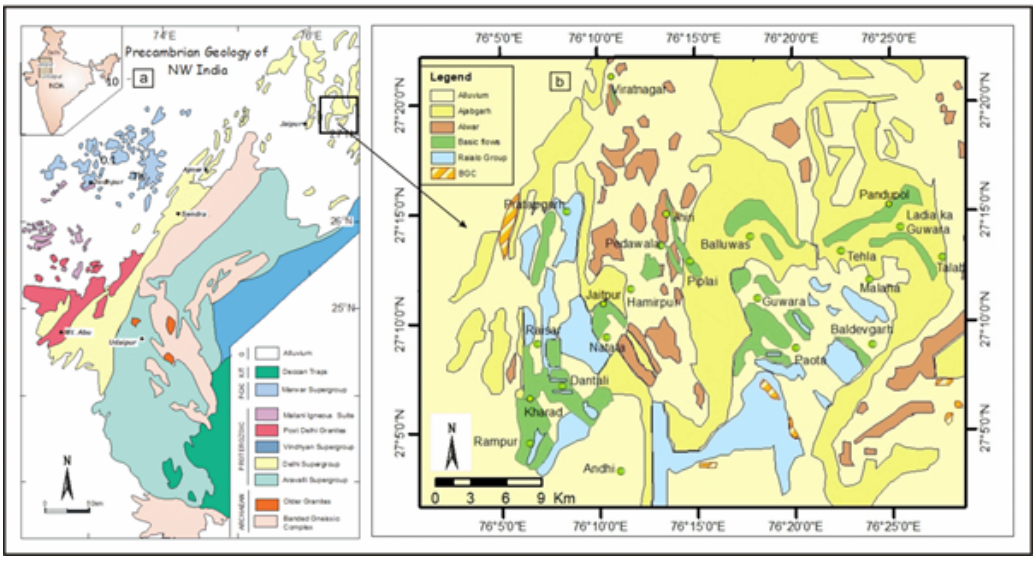

Figure 1. (a) Simplified geological map of Aravalli Delhi Fold Belt (**Vanlenteetal2009**). (b) Lithostratigraphic map of Alwar sub-basin (adapted from (Sing, 1988)).

introduced the terms North Delhi Terrane (NDT) and South Delhi Terrane (SDT) for Delhi rocks in a purely geographic context. The ADMB bears evidence of syn-sedimentary volcanism and subsequent emplacement of granitic plutons. Crawford (1970) and Heron (1917, 1922) and Heron (1953) assigned a Pre-Delhi (*System*) age to these granitoids.

The erstwhile Delhi System was initially subdivided into Alwar Series (older) and Ajabgarh Series (younger) by Heron (1917, 1953) who also proposed an independent stratigraphic status to the Raialo Series, between Aravalli and Delhi systems. During a major revision of the stratigraphy of the Aravalli Craton, Gupta et al. (1980) and Gupta et al. (1997) included Raialo rocks into the realm of the Delhi Supergroup as its basal stratigraphic unit.

Sedimentation in the NDFB can be resolved into three NE-trending sub-parallel, spatially distinct basins, namely, the Khetri, Alwar, and Lalsot-Bayana sub-basins, from west to east (Sinha-Roy et al., 1998). The geological sequence of the Delhi Supergroup and its tripartite subdivision into the Raialo (carbonate and basic volcanic rocks), Alwar (arenaceous facies), and Ajabgarh (argillaceous-arenaceous facies) groups holds true for the NDFB, however, such grouping cannot be applied to the SDFB (Gupta et al., 1980; Gupta et al., 1997; I, 2001).

The Raialo Group is a predominantly carbonate-arenaceous facies ensemble in the basal part and mafic meta-volcanic rocks in the upper part. The overlying Alwar Group represents a dominantly arenaceous facies sequence, further subdivided into the Rajgarh, Kankwarhi, and Pratapgarh formations (Chakrabarti et al., 2004). The Ajabgarh Group represents the youngest stratigraphic unit of NDFB and consists of argillic-arenaceous and calcareous components (Singh, 1984). The Ajabgarh Group is subdivided into Kushalgarh, Sariska, Thanaghazi and Bharkol formations, in the order of decreasing geological age. The stratigraphic succession of the Delhi Supergroup of rocks in the Alwar sub-basin, (Chakrabarti et al., 2004), is given in Table 1.

Several granitic bodies are known from the NDFB and were considered syn-orogenic, S-type intrusions into Delhi rocks for a long time (Chaudhary et al., 1984). However, Pandit and Khatatneh (2003) discovered and reported A-type signatures in Alwar sub-basin granitoids. Later, the A-type granitoids were also described by Kaur et al. (2007) and Kaur et al. (2011) in the Khetri sub-basin. In addition, these authors also noted arc signatures in some of the Khetri sub-basin granitoids. Geochronological studies during the last decades have assigned Paleoproterozoic age for these NDFB granitoids (Biju-Sekhar et al., 2003; Kaur et al., 2007; Kaur et al., 2011). The geochronological distinction between the northern and southern domains of the Delhi Supergroup granitoids has been substantiated in several later studies that reiterate that the NDFB ∼1.75 Ga; (Kaur et al., 2011; Kaur et al., 2016; Pandit et al., 2021) is significantly older than SDFB (Deb et al., 2001; Pandit and Khatatneh, 2003; Singh et al., 2010; Mckenzie et al., 2013; Wall et al., 2018). Kaur et al. (2007) suggested < 1660 Ma depositional age for Delhi sedimentation in the NDFB. The detrital zircon U-Pb age-based study by Wang et al. (2017) postulated a 1720 Ma depositional age for the North Delhi sediments, further supporting a diachronous sedimentation history for the Delhi Supergroup.

2.2 Geology of the study area

This study focuses on the Raialo Group mafic volcanic rocks from the Alwar sub-basin of the NDFB and the study area is shown in Fig. 1 b. In this region, sediments and syn-

Table 1. Stratigraphic succession of the Delhi Supergroup of rocks in the Alwar sub-basin as summarized by Chakrabarti et al. (2004).

Post Delhi		Intrusive granite
Delhi Supergroup	Ajabgarh Group	Arauli Formation
		Bharkol Formation
		Thana-Ghazi Formation
		Seriska Formation
		Kushalgarh Formation
	Alwar Group	Pratapgarh Formation
		Kankwarhi Formation
		Rajgarh Formation
	Raialo Group	Tehla Formation
		Serrate Formation
		Dogeta Formation
.....Unconformity.....		
Basement Mangalwar Complex (BGC)		

sedimentary mafic volcanic rocks (since metamorphosed) were deposited over an Archean basement that mainly comprises granite gneiss of Mangalwar Complex (Bhilwara Supergroup/Banded Gneiss Complex). The exposures of basement rocks are scanty and could be observed only at a few places, in the form of ground-level exposures of granite gneiss, garnet-sillimanite schist, banded magnetite quartzite, quartz-chlorite schist, talc-schist, silicified quartzite, etc. The Raialo Group has been subdivided into three formations and is unconformably overlain by the Alwar Group rocks. The hiatus in sedimentation between the two groups is represented by the development of a (basal) conglomeratic horizon that constitutes the basal unit of the Alwar Group. The lowermost unit of the Raialo Group, the Dogeta Formation, is represented by impure marble and patches of gritty quartzite. Serrate Formation, the middle unit, mainly contains massive quartzite. Tehla Formation, the uppermost unit of the Raialo Group, is represented mainly by mafic meta-volcanic flows, quartzite, and schist with sporadic exposures of feldspathic quartzite (Banerjee and Singh, 1977). The Raialo Group rocks show evidence of greenschist to amphibolite facies metamorphism, as inferred from the mineral assemblages (details provided in the following section). The lithological succession of the Raialo Group in the study area is given in Table 2.

In the study area, steep quartzite ridges constitute the high-elevation topography, while granite-gneiss basement rocks are generally covered under the vast alluvium. Mafic metavolcanic rock outcrops, a few meters to $>$ 100 m in thickness, were sampled from Pandupol, Tehla, Rampur, Kharad, Dantali, Natata, Jaitpur, Hamirpur, Jhiri, and Viratnagar area where they occur as series of small hillocks and ground-level exposures. In places, they are exposed along the lower flanks of quartzite ridges. The mafic metavolcanic rocks are mainly fine- to medium-grained, massive to foliated and dark greenish in color. They show greenschist to amphibolite facies metamorphism and polyphase deformation, reflected in the development of brown streaks (iron oxide leaching) and secondary minerals. Banerjee and Singh (1977) delineated a total of 16 flows from the region. Despite metamorphism, deformation, and notable alteration these rocks occasionally display pristine magmatic features, such as well-preserved pillow lava structures with diagnostic glassy rinds and radial cracks, recently reported from a solitary site near Tehla (Bairwa and Pandit, 2021), and subrounded vesicles, at times, partly filled with secondary quartz and calcite.

3. Petrographic and mineralogical characteristics of the raialo metavolcanic rocks

The petrographic examination of the sampled mafic metavolcanic rocks shows significant textural and mineralogical variations. Major minerals present in these rocks are amphibole (mainly hornblende), plagioclase, microcline, biotite, and chlorite with minor epidote, quartz, sphene, zircon, Fe-Ti oxide, etc. Relict pyroxene could also be seen in some cases. Based on the textural and mineralogical criteria, these rocks can be classified into four sub-groups, namely (a) hornblende-biotite schist, (b) chlorite-actinolite schist, (c) hornblende schist and (d) amphibolite.

3.1 Hornblende-biotite schist

These rocks, exposed around Pandupol and Viratnagar area, are fine- to medium-grained, foliated, and dark gray to greenish-black in color. Their thin section examination reveals the presence of hornblende, biotite, plagioclase, quartz, and epidote as the main minerals, while zircon, chlorite, and Fe-Ti oxides represent the accessory mineral phases. At places, deformed and recrystallized titanite (sphene) can also be seen. Epidote and chlorite represent alteration products of plagioclase and biotite, respectively (Fig. 2 a).

3.2 Chlorite-actinolite schist

These are medium- to coarse-grained, gray to greenish-gray rocks, exposed as small isolated hillocks around Rampur, Dantali, and Kharar villages. Their petrographic examination shows a preferred orientation of actinolite, imparting a 'flow texture' to the rock. Some of the actinolite grains also display a sieve structure (Fig. 2 b). The major minerals are chlorite and actinolite while plagioclase and quartz are present in subordinate amounts.

3.3 Hornblende schist

The hornblende schist occurs as low-lying outcrops occupying the lower flanks of quartzite ridges around Natata, Jaitpur, and Hamirpur villages as fine- to medium-grained and gray to greenish-gray colored rocks. They display a well-developed schistosity, therefore, named hornblende schist. Their petrographic examination reveals hornblende

Table 2. Stratigraphic succession of the Raialo Group in the study area (Gupta et al., 1992; Rastogi et al., 2016).

Raialo Group	Tehla Formation	Quartzite, schist and intercalated Sequence of quartzite and metabasic
	Serrate Formation	Quartzite
	Dogeta Formation	Tremolitic marble, quartzite phyllite and metabasic bands within impure marble
		————Unconformity———
		Mangalwar Complex (BGC)

as the most dominant mineral, with the characteristic prismatic habit, greenish to pale green pleochroism, and two sets of cleavages intersecting at 120°/60° (Fig. 2 c). The other minerals are plagioclase and minor quartz.

3.4 Amphibolite

The mafic meta-volcanic rocks exposed around Tehla and Jhiri area are also amphibole dominant and named amphibolite. These rocks in the Tehla area are fine-grained, greenish-black in color, and occur as massive to vesicular flows. At places, vesicles are filled with secondary quartz and calcite. Well-preserved pillow lava structures were recently reported from the Tehla metavolcanic rocks by Bairwa and Pandit (2021), who also provided details on the pillow morphology and pillow dimensions. Petrographic examination of these rocks reveals hypocrystalline to sub-ophitic texture and actinolite-tremolite as the major minerals along with minor quartz and plagioclase (Fig. 2 d). The meta-volcanic rocks of the Jhiri area contain moderate-size hornblende and actinolite grains, set in a fine-grained groundmass constituted by quartz and altered plagioclase (Fig. 2 e). Tiny, high-relief grains, mainly epidote (sausserite) and sericite (Fig. 2 f) were also observed. Well-defined schistosity in these rocks can be attributed to the parallel alignment of amphibole minerals.

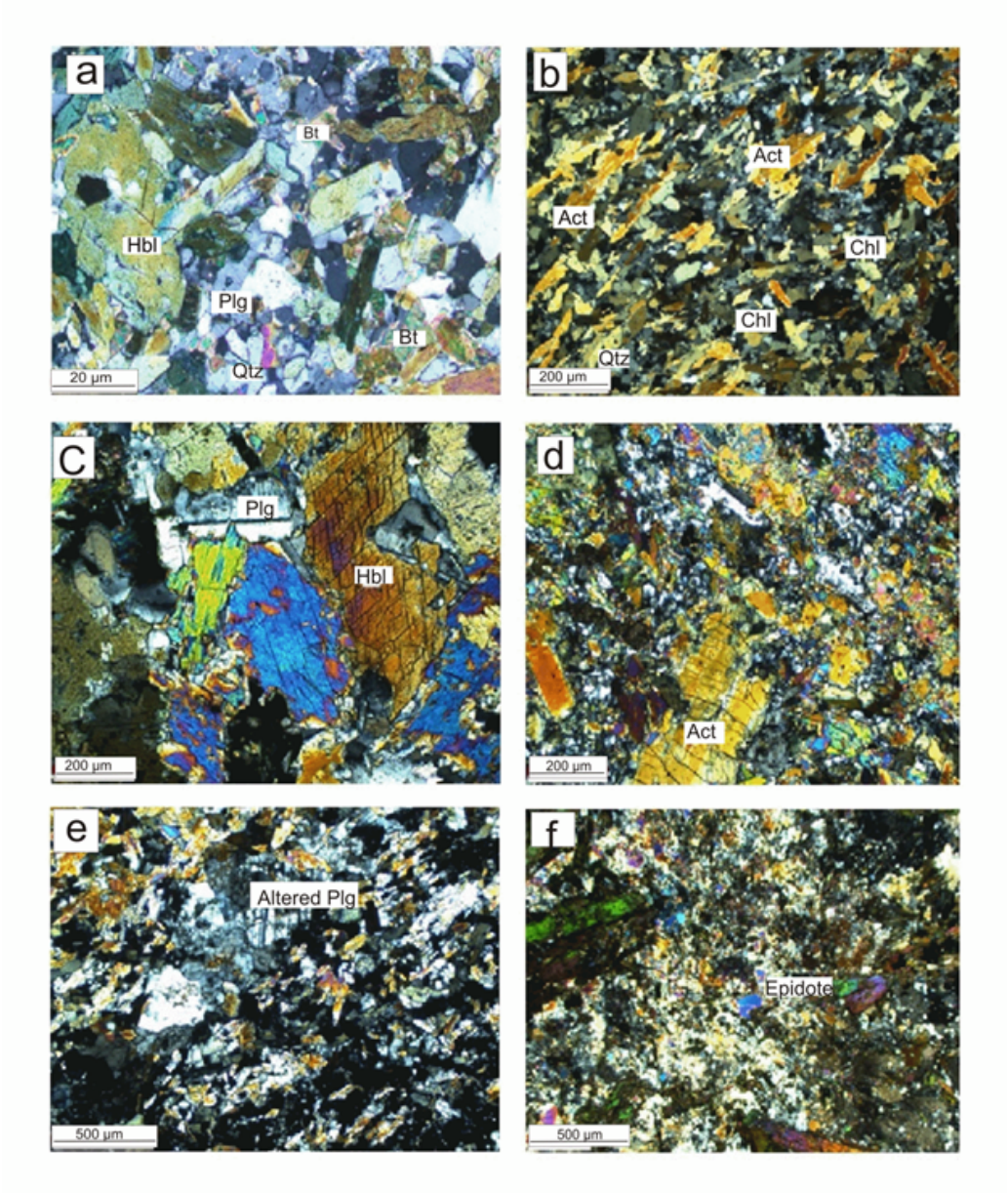

Figure 2. Photomicrographs of the Tehla mafic metavolcanic rocks (a) showing alteration of hornblende to biotite and plagioclase to epidote, (b) chlorite and actinolite laths defining schistosity along with minor plagioclase and quartz, (c) hornblende grains showing two sets of cleavage intersecting at $120^0/60^0$, (d) sub-ophitic texture and actinolite and tremolite occurring as major minerals, (e) plagioclase laths showing sieve and skeletal texture, (f) amphibole grains replaced by chlorite and epidote (sausserite), and minor quartz and altered plagioclase (sericite) in the groundmass. Mineral abbreviations: Qtz: Quartz, Plg: Plagioclase, Bt: Biotite, Act: Actinolite, Chl: Chlorite, Hbl: Hornblende.

4. Sampling and analytical methods

Fresh and visibly unaltered representative samples of mafic meta-volcanic rocks were collected from several locations. Each sample was broken into centimeter-size chips and those showing alteration stains and weathering effects were rejected before powdering the rest to -200 mesh size. A total of 31 representative samples were subjected to whole-rock major oxide and trace element analyses using SIEMENS SRS-3000 X-ray fluorescence spectroscope (Saini et al., 2007) while REE analysis was carried out by (ELAN-DRC-E) ICP-MS, both housed at the Wadia Institute of Himalayan Geology, Dehradun (Khanna et al., 2009). Reported analytical precision is better than $\pm 7\%$ for major oxides and trace elements. For further details on the analytical procedure, please refer to Saini et al. (2007) and Khanna et al. (2009).

5. Whole-rock geochemistry

5.1 Geochemical classification

The analyzed mafic metavolcanic rocks display a wide range of SiO_2 (48.23-53.93 wt. %), MgO (5.10-11.58 wt. %), Al_2O_3 (9.64 - 12.91 wt. %), K_2O (0.09 - 1.32 wt. %) (except a lone sample with an anomalous value of 2.23 wt.%), CaO (4.13 - 12.31 wt. %) and TiO_2 (0.50 - 3.25 wt. %) contents. The transitional elements display moderate to low concentrations (Ni – 16 to 86 ppm; Cr – 44 to 182 ppm; Co - 36 to 58 ppm). The low LOI values ($< 1\%$) of these rocks suggest that they may not be significantly weathered, while low Rb/Sr ratios (0.01 - 0.19) further suggest that the chemical characteristics may not have been significantly modified during the post-crystallization process(es). Although the trace presence of titanite in hornblende biotite schist can be attributed to the high Ti content, the geochemical characteristics of the other petrographic types do not show any notable correspondence between petrography and geochemistry. Therefore, the geochemical characteristics of the entire data set have been described together in this section.

The Ti is one of the least mobile elements and an important denominator for working out the basalt petrogenesis and discriminating the tectonic setting of magmatism (Rollinson, 1993). Considering its relative immobility during the post-crystallization processes, we assume that the TiO_2 concentrations in these low-grade metamorphic rocks represent primary geochemical signatures. Studied mafic metavolcanic rocks show a wide variation in TiO_2 abundance and display an inverse correlation with MgO, another significant index for evaluating the crystallization behavior of basaltic magmas. Therefore, the rocks have been tentatively subdivided in to three geochemical types, based on the relative abundance of TiO_2 and Mg#. We have used Mg# instead of absolute MgO content because it includes two parameters (Fe and Mg).

1. Low Ti ($TiO_2 < 1$ wt. %) – high Mg# (Average – 58.24, Range – 51.12 – 66.48) group
2. Moderate Ti ($TiO_2 = 1$–2 wt. %) – moderate Mg# (Average – 55.03, Range - 43.04 – 64.43) group, and
3. High Ti ($TiO_2 > 2$ wt. %) – low Mg# (Average – 51.18, Range – 46.59 – 55.98) group

The average geochemical data for each group and the range of each parameter are listed in Table 3. Since this is the first study on geochemical characteristics of Tehla metavolcanic rocks, the data from the Bayana and Alwar sub-basins of the North Delhi Fold Belt and Aravalli basic volcanics (Ahmad and Tarney, 1994; Abu-Hamatteh, 2002; Raza et al., 2014) have also been included for comparison and overview of Proterozoic mafic magmatism in the Aravalli Delhi Fold Belt.

In the most widely used Total Alkali versus Silica (TAS) classification scheme of Bas et al. (1986) the Raialo metavolcanic rocks, despite a variation in Ti – Mg contents, display an overall subalkaline/tholeiitic affinity and plot as a single coherent group across the basalt-basaltic andesite fields (Fig. 3 a). Other samples also show a broad subalkaline/tholeiitic character, however, with a data scatter. Although the low LOI values of the Raialo mafic metavolcanic rocks (Table 3) suggest an insignificant weathering and least geochemical alteration effect, the possibility of modification in the alkali contents needs to be thoroughly evaluated on account of their highly mobile nature. Therefore, the samples were further classified using the relatively immobile elements-based.

geochemical classification (Nb/Y vs. Zr/ TiO_2) scheme of Winchester and Floyd (1977). The diagram is in general agreement with the TAS classification, however, the three groups define a tight cluster in the sub-alkaline basalt domain and there is an overall coherence with the other data from the Aravalli Delhi Fold Belt (Fig. 3 b). A general agreement between major oxide and trace element based classifications points toward an insignificant post crystallization alteration effect. The classification scheme of Jensen (1976) utilizes Fe+Ti, Al, and Mg, which are important parameters in evaluating magmatic differentiation. In this diagram, the high Ti –low Mg and low Ti –high Mg samples show clear discrimination and plot in high Fe and high Mg tholeiite fields, respectively while the moderate Ti group plots at the boundary between the two fields (Fig. 3 c). The Aravalli samples, on account of high Mg contents, plot in the komatiitic basalt and komatiite fields, distinctly away from the rest of the data set. The Raialo mafic metavolcanic rocks define an iron enrichment trend and tholeiitic affinity in the AFM plot of Irvine and Baragar (1971).

5.2 Trace and rare earth elements geochemistry

Trace and Rare Earth Elements, although collectively accounting for less than 1% of the bulk rock, are significant in evaluating the magma generation and its evolution. The multi-element spider diagrams wherein trace elements are arranged according to increasing degree of compatibility, provide an overview of the relative abundance of critical trace elements, therefore, are useful in understanding the geochemical characteristics of the rock during the magma evolution process (Wilson, 1989; Rollinson, 1993). The primordial-mantle (PM) normalized spider diagrams for the three groups of Raialo mafic metavolcanic rocks are presented in Fig. 4 a (normalizing values after (Sun and McDonough, 1989)); the data for Bayana and Alwar sub-basins (Raza et al., 2014), other NDFB and Aravalli volcanic, have

Table 3. Major oxides (wt %), Trace and Rare Earth Elements (ppm) data of mafic metavolcanic rocks of Raialo Group of North Delhi Fold Belt. The average values of Bayana and Alwar volcanics (Raza et al., 2014), Aravalli volcanics (Ahmad and Tarney, 1994) and Aravalli-Delhi volcanics (Abu-Hamatteh, 2002) have also been shown for comparison. (TH*, Tholeiite; KM*, Komatiite; KB*, Komatiitic basalt).

Elements	Low Ti-High Mg (n=14)		Moderate Ti-Moderate Mg (n=14)		High Ti-Low Mg (n=03)		Alwar volcanics (Raza et al., 2014)	Bayana volcanics (Raza et al., 2014)	Aravalli volcanics (Ahmad and Tarney, 1994)			Aravalli-Delhi volcanicds (Abu-Hamatteh, 2002)	
	Avg.	Range	Avg.	Range	Avg.	Range	Avg.	Avg.	TH*	KM*	KB*	Jharol belt	Ambaji Deri
SiO_2	51.25	49.11-53.54	51.08	49.17-53.93	50.36	48.23-51.64	49	51.89	53.26	52.15	53.61	47.92	49.35
TiO_2	0.88	0.50-1.00	1.39	1.01-1.73	2.7	2.04-3.25	1.06	1.51	1.46	0.45	1.125	1.45	1.74
Al_2O_3	11.5	10.06-12.51	11.58	9.64-12.91	11.02	10.22-11.84	12.55	11.31	13.11	5.2	9.33	12.32	13.37
Fe_2O_3	13.68	12.29-15.35	14.85	13.13-17.19	16.08	14.34-17.60	15.44	15.2	13.88	10.77	12.78	12.79	13.04
MnO	0.19	0.18-0.22	0.18	0.09-0.25	0.13	0.12-0.17	0.2	0.21	0.21	0.23	0.25	0.2	0.26
CaO	9.96	6.54-12.31	7.57	5.92-9.79	6.3	4.13-8.62	9.01	7.44	7.81	10.21	8.9	12.08	10.61
MgO	8.35	6.61-11.58	8.09	5.10-10.56	7.38	5.37-8.91	8.05	8.37	6.29	20.08	11.25	10.17	7.63
Na_2O	2.18	1.15-3.78	2.52	1.59-3.53	2.47	1.91-3.30	3.39	1.92	3.02	0.32	2.21	1.77	1.59
K_2O	0.18	0.13-0.24	0.79	0.09-2.34	0.95	0.57-1.32	0.15	1.48	0.97	0.06	0.2	0.46	1.17
P_2O_5	0.08	0.05-0.12	0.147	0.07-0.20	0.36	0.22-0.54	0.11	0.17	0.15	0.04	0.12	0.14	0.28
La	4.43	2.40-6.25	10.23	2.28-29.13	22.08	8.50-35.27	3.72	17.52	15.42	4.75	17.11	–	18.63
Ce	10.91	5.76-14.93	24.32	9.37-51.07	50	28.41-71.95	10.08	34.24	38.8	12.56	38.53	11.17	44.12
Pr	1.64	1.09-2.27	3.21	1.34-6.02	7.09	4.02-10.53	1.3	4.14	4.85	1.44	4.7	–	–
Nd	7.89	4.80-10.52	14.93	7.08-25.50	33.92	19.40-50.49	8.04	17.15	19.48	5.95	18.12	13.76	27.96
Sm	2.36	1.38-2.96	3.86	2.64-5.17	8.2	5.45-11.80	2.26	4.03	4.81	1.74	4.16	5.76	7.21
Eu	0.83	0.53-1.08	1.34	0.93-1.69	2.48	1.59-3.40	0.79	1.28	1.48	0.48	1.26	2.06	1.95
Gd	2.86	1.64-3.65	4.36	2.91-6.31	8.43	6.06-11.99	3.21	3.78	5.06	1.97	4	6.27	7.58
Tb	0.54	0.29-0.72	0.81	0.61-1.09	1.51	0.94-2.27	0.57	0.61	–	–	–	–	–
Dy	3.48	1.88-4.64	5.03	3.97-6.93	8.75	5.22-13.44	3.42	3.19	4.76	1.97	3.25	7.39	7.51
Ho	0.73	0.41-0.96	1	0.78-1.50	1.64	1.02-2.55	–	–	–	–	–	–	–
Er	2.09	1.12-2.86	2.93	2.24-4.02	4.7	2.55-7.53	2.35	1.98	2.69	1.14	1.58	4.28	4.45
Tm	0.32	0.18-0.44	0.44	0.32-0.61	0.68	0.37-1.10	–	–	–	–	–	–	–
Yb	2.1	1.13-2.76	2.87	2.00-3.94	4.28	2.38-6.98	2.09	1.56	2.29	1.26	1.25	4.94	4.16
Lu	0.3	0.17-0.42	0.42	0.28-0.57	0.62	0.33-1.02	0.31	0.21	0.32	0.2	0.16	0.66	0.57
U	0.57	0.52-0.62	0.79	0.52-1.16	1.54	1.13-1.95	–	–	–	–	–	–	–
Ba	88.04	20.00-371.01	199.67	32-550.29	205.84	178-233.68	1	242.57	250.9	5	36.16	31.25	345.22
Co	52.42	48.00-58.00	51	41-59	42.33	36-52	81.25	33	–	–	–	–	–
Cr	142.21	97.00-175.00	104.64	44-182	102.33	69-143	139	237.62	256.4	2748.33	1077.5	442.5	125.33
Cu	85.96	28.00-162.04	47.02	4.78-162.53	60.97	8.00-153.90	–	–	–	–	–	–	–
Ga	12.95	9.35-19.00	18.48	11.80-24	24.5	21.51-27	–	–	22.8	10.66	11.83	20	21.11
Nb	5.12	2.40-9.00	9.42	4.80-13	21.46	10.4-29	16	10.25	7	4.16	7	15.25	10.55
Ni	75.78	58-86	50.21	16-81	48.33	17-69	41.75	78.5	98.8	1198.5	318.33	184.25	92.44
Pb	4.75	1- 21.70	7.46	1.20-15	6.63	0.9-12	–	–	–	–	–	–	–
Sc	45.28	41-50	41.71	30-50	37.33	30-45	–	–	–	–	–	–	–
Sr	125.14	84-166	142.5	64-29	165.33	108-235	91.37	194.37	168.6	12.16	76.83	308.5	226.22
V	291.78	237-342	337.92	267-452	365	326-420	–	–	265.9	108	191.33	257.5	307.11
Y	19.21	23-Dec	27	19-36	37.66	30-49	22.87	21.37	27.3	13	17.83	34.25	44.77
Zn	93.35	73-128	106.42	30-186	78.33	39-148	–	–	152.2	122.83	152.16	–	330.25
Zr	53.71	28.00-67.00	98.5	56-164	200	132-276	66.62	86	145.7	49.5	109.67	108.75	192.33
Th	1.49	1.13-1.96	3.672	1.05-6	3.01	3.01-3.01	1	1.96	5.1	6.83	5.83	–	–
Rb	2.09	1.00-6.00	27.1	Feb-85	28.33	May-47	2.5	25.12	30.4	2.5	6.67	7.75	49.88
Be	0.43	0.35-0.58	0.68	0.47-0.88	1.86	1.34-2.39	–	–	–	–	–	–	–
Ge	1.35	1.21-1.41	1.38	1.20-1.57	1.45	1.42-1.49	–	–	–	–	–	–	–
Sn	<1	–	1.89	1.29-3.22	4.61	2.32-6.91	–	–	–	–	–	–	–
Hf	1.66	1.33-2.11	3.1	1.86-4.74	7.46	5.87-9.06	–	–	–	–	–	–	–
Ta	0.21	0.21-0.23	0.45	0.24-0.58	1.43	1.14-1.73	0.8	1.08	–	–	–	–	–

2008-8779[https://dx.doi.org/10.57647/j.ijes.2024.1603.13]

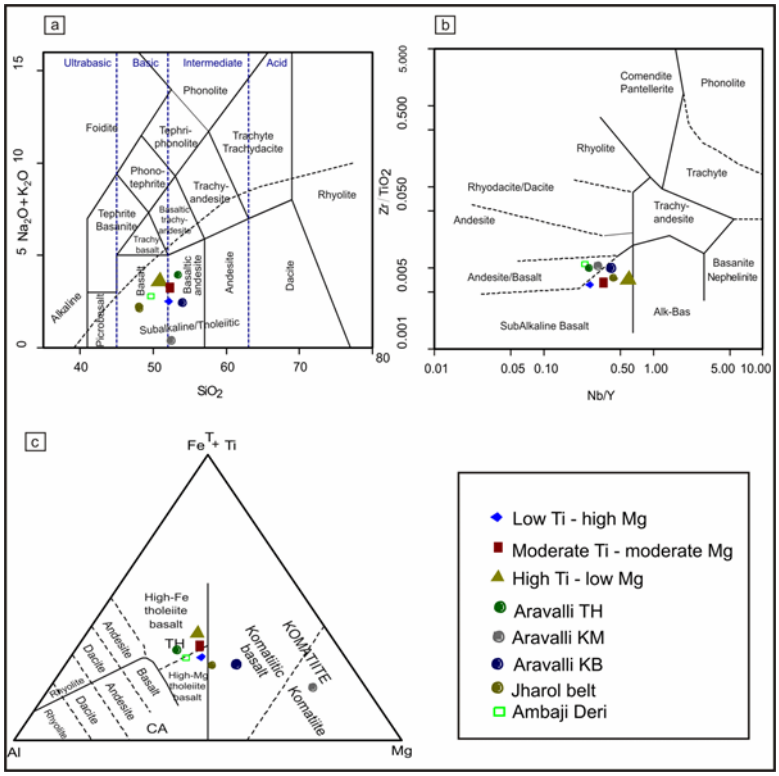

Figure 3. Geochemical classifications of the Tehla metavolcanic rocks based on (a) Total Alkali vs. Silica (TAS) (Bas et al., 1986), (b) Nb/Y vs. Zr/ TiO_2 (Winchester and Floyd, 1977) and (c) Fe+Ti, Al and Mg (Jensen, 1976) classifications schemes. Aravalli TH (tholeiite); KM (komatiite); KB (komatiitic basalt) - Ahmad and Tarney (1994); Jharol belt and Ambaji Deri - Abu-Hamatteh (2002) have also been shown for comparison.

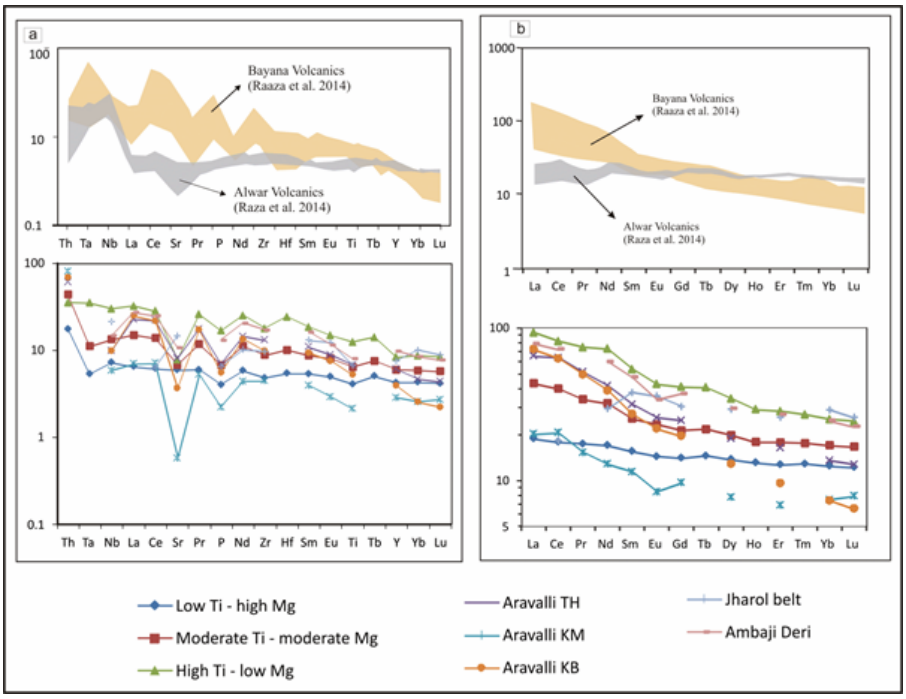

Figure 4. (a) Primordial-mantle (PM) normalized trace element spider diagrams of the Raialo metavolcanics (normalizing values after (Sun and McDonough, 1989)). (b) Chondrite normalized REE diagrams of the Raialo metavolcanics (normalizing values after (Sun and McDonough, 1989)). An overview of Bayana and Alwar volcanics (Raza et al., 2014); Aravalli TH (tholeiite); KM (komatiite); KB (komatiitic basalt) - Ahmad and Tarney (1994); Jharol belt and Ambaji Deri - Abu-Hamatteh (2002) have also been shown for comparison.

also been plotted for comparison. Although the three groups show an overall general slope towards the right side of the diagram, notable differences among them are discernible in terms of enrichment and depletion levels of individual elements. The low-Ti samples display Th enrichment, minor Ta depletion, and a small Ti negative anomaly. The moderate Ti group samples show similar trends but higher enrichment levels for the incompatible trace elements. In the absence of any discernible Nb anomaly, the Sr depletion and Th enrichment do not seem to be caused by crustal input and Sr depletion can be linked to plagioclase crystallization. The compatible trace elements show relatively lower enrichment levels in all the samples and lack any notable anomalies. The high-Ti (low-Mg) samples are distinct from the rest in terms of significant LILE enrichment, a common feature of evolved magmas. This group displays a rather smooth trend, except for minor negative anomalies for P and Zr. A positive Th anomaly and lack of Ti and Nb–Ta negative anomalies, preclude any crustal contamination for these rocks. It is interesting to note that all three groups display a variable Pb enrichment. The behavior of Pb in basaltic melts could be intriguing and difficult to explain. It may be an inherent characteristic of the magma. Available trace and Rare Earth Element data for Aravalli mafic metavolcanic rocks have also been plotted (Fig. 4 a, 4 b) but it is hard to make any meaningful comparison as some parameters are missing.

The REE data are conventionally normalized against chondrite values and in the present case, the normalized REE concentrations (normalizing values after (Sun and McDonough, 1989)) are plotted in Fig. 4 b. The chondrite normalized REE patterns of the Low–Ti (high-Mg #) volcanic rocks show a flat trend and moderate enrichment (15 to 20 times Chondrite) with no visible anomalies, therefore representing the undifferentiated melt compositions. The medium-Ti group displays moderate LRRE enrichment (La, ∼60 times chondrite) and generally flat HREE trends, implying a moderately differentiated melt while the high-Ti group shows a relatively steep LREE slope (La, ∼95 times chondrite) and sub-horizontal HREE trends.

6. Discussion on melt source and tectonic setting

A close similarity between low- and moderate-Ti samples is indicated by their significant Th enrichment and minor Ta and Ti depletion. These geochemical attributes underline a genetic relationship between the two groups. Minor Zr depletion and decoupling between the Nb–Ta pair rule out any significant crustal input in these rocks, therefore, their high Th abundance seems an intrinsic character derived from the parent rock (Fig. 4 a). In the TiO_2 – MgO diagram, the Raialo Group mafic metavolcanic samples define an inverse correlation (Fig. 5 a). This attribute is also replicated in the samples from Aravalli–Delhi Belt (Ahmad and Tarney, 1994; Abu-Hamatteh, 2002). The low-, moderate-, and high-Ti groups show an inverse correlation between the CaO – P_2O_5 pair which is a normal attribute of basaltic magma differentiation. The P behaves incompatibly in basaltic magma evolution and would show progressive enrichment while CaO would decrease (Fig. 5 b).

The REEs are considered generally immobile during post-crystallization processes and low-grade metamorphism, therefore, constitute a more robust data set for deciphering the process of magma generation and its evolution. The low-Ti group samples show flat and slightly enriched REE trends, the absence of any LREE/HREE fractionation, and lack of Eu anomaly (Fig. 3 b). These characteristics suggest an undifferentiated primary melt derived from an enriched mantle source with no residual garnet (Fig. 4 b). During progressive fractional crystallization, the low–Ti melt differentiated and evolved into the medium-Ti basalt through enrichment of Ti and LREE, and depletion of Mg (early removal of Mg-bearing mineral phases). Both groups display flat HREE patterns with closely comparable enrichment levels. The high-Ti group shows the highest trace element abundances (Fig. 4 a) and also has the highest ΣREE and highest LREE enrichment (Fig. 4 b). However, their distinct trace element characteristics, such as lack of Th anomaly, Nb – Ta coupling, etc., rule out any genetic relationship with either low- or medium Ti group rocks. Thus this group represents derivation from an enriched mantle source, distinct from the other groups. The high-Ti group may represent either a temporally distinct event or a heterogeneous mantle source, and melting at a relatively shallow depth.

The TiO_2 – MnO – P_2O_5 triangular diagram (Mullen, 1983) is useful in discriminating the tectonic setting of mafic magmatic rocks. In this diagram, the low-Ti group shows an Island Arc Tholeiite (IAT) affinity, grading towards the MORB field for the medium Ti group, further substantiating a close linkage between the two groups (Fig. 6 a). On the other hand, the high-Ti group plots in the OIT field, as a separate group. In the Ti–Zr discrimination diagram of Pearce (1982) the low-Ti group shows Island Arc lava characteristics, transitional into the within plate lava field while the high-Ti group plots clearly away, in the within plate field (Fig. 6 b). In a recent update of their earlier trace element discrimination scheme, Pearce et al. (2021) proposed a Th/Yb – Nb/Yb diagram wherein low- and medium-Ti groups indicate an E-MORB like source, affected by fluid interaction under arc setting (Fig. 6 c) while the high-Ti group shows affinity with an uncontaminated E-MORB like source. The Bayana sub-basin volcanics represent more evolved compositions with source regions significantly affected by fluid interaction. The Nb/La values of the high-Ti group show a close affinity with PM while low- and medium-Ti groups can be linked through La enrichment and Mg depletion during progressive differentiation (Fig. 6 d).

7. Conclusion

The geochemical characteristics of the Raialo Group mafic metavolcanic rocks of the southern Alwar sub-basin, discussed above, lead to the following conclusions:

1. The TiO_2 and Mg# of mafic metavolcanic rocks allow their subdivision into three geochemical groups, namely; low-Ti – high-Mg#, moderate-Ti – moderate-Mg#, and high-Ti – low-Mg# basalts.
2. The low-Ti (high Mg#) group represents the early melt compositions that eventually evolved into moderate-Ti

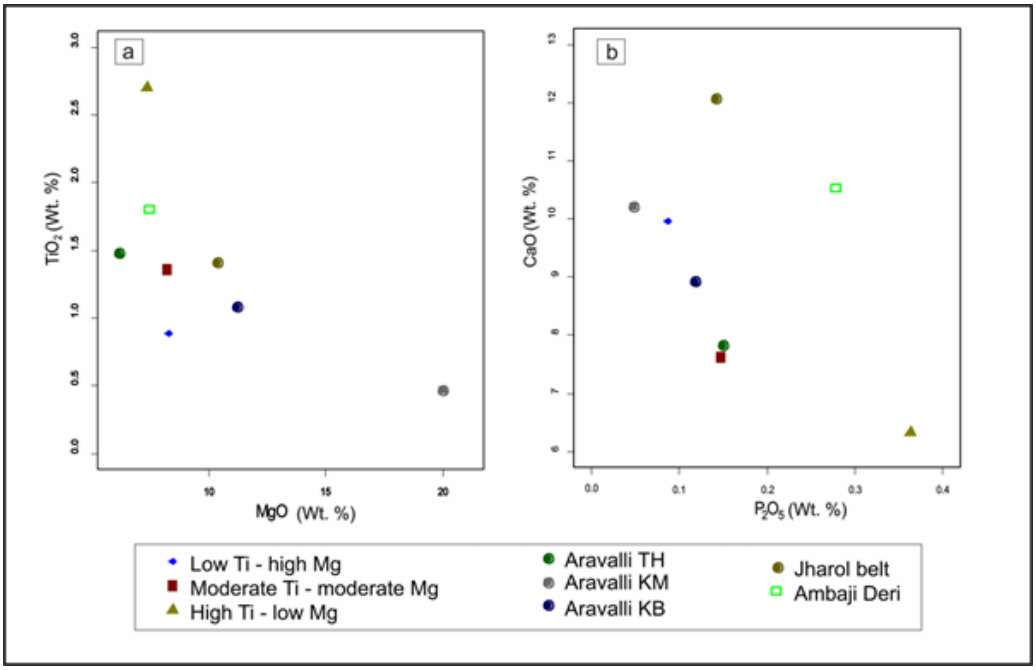

Figure 5. (a) MgO vs. TiO_2 and (b) CaO vs. P_2O_5 binary plots showing an inverse correlation between the two elemental pairs. Aravalli TH (tholeiite); KM (komatiite); KB (komatiitic basalt) - Ahmad and Tarney (1994); Jharol belt and Ambaji Deri - Abu-Hamatteh (2002).

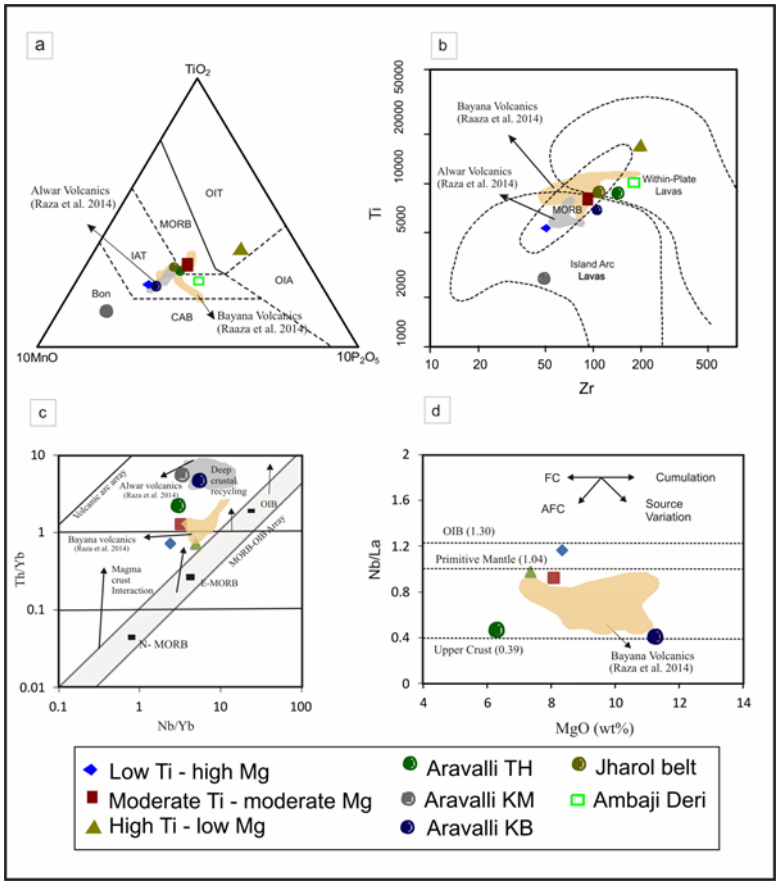

Figure 6. Tectonic discrimination diagrams of basic metavolcanic rocks of the Tehla Formation (a) TiO_2-MnO-P_2O_5 ternary diagram (Mullen, 1983) (b) Zr vs. Ti diagram (Pearce, 1982) (c) Th/Yb vs. Nb/Yb diagram (Pearce et al., 2021) (d) Nb/La vs. MgO diagram (Kepezhinskas et al., 1996); Aravalli TH (tholeiite); KM (komatiite); KB (komatiitic basalt) - Ahmad and Tarney (1994); Jharol belt and Ambaji Deri - Abu-Hamatteh (2002) have also been shown for comparison.

basalts during progressive fractionation.
3. Although the high-Ti group represents the most evolved magma composition, its distinct geochemical signatures preclude any genetic relationship with low- and moderate-Ti groups. Therefore, the high-Ti samples represent evolution from a distinct and more evolved mantle source and do not show any crustal input. The crustal input in the other two groups could not be evaluated due to contradictory geochemical signatures such as Th enrichment, absence of Nb anomaly, and minor Zr depletion.
4. The geochemical discrimination patterns point toward a primitive mantle source modified by fluids for the low-Ti group, and transitional setting for the medium-Ti group while the high-Ti group shows affinity with the within-plate setting.
5. The low- and medium-Ti groups show a close geochemical affinity and genetic linkage with each other while the high-Ti group represents a discrete (enriched) mantle source, thus underlining either mantle heterogeneity or different depths of mantle melting, if they erupted at the same time.

Acknowledgement The authors express their gratitude to Shri Shailendra Singh, Director, GSI, Northern Region, Lucknow, and Dr. A.K. Singh, Scientist-E, WIHG, Dehradun for their encouragement and support. We would like to thank Prof. H. Mollai for his comments and valuable suggestions on an earlier version that have greatly improved the presentation and interpretation. We also thank four anonymous reviewers for their comments that have significantly contributed to improving the paper.

Authors Contributions
All authors have contributed equally in preparing the paper.

Availability of Data and Materials
Data is available on request from the authors. The data supporting this study's findings are available from the corresponding author, upon reasonable request.

Conflict of Interests
The authors declare that they have no known competing financial interests or personal relationships that could have appeared to influence the work reported in this paper.

References

Abu-Hamatteh Z. S. H. (2002) Geochemistry and tectonic framework of proterozoic mafic metavolcanics of aravalli-delhi orogen, nw india. *Chem. Erde.* 62:123–144. https://doi.org/10.1078/0009-2819-00016

Abu-Hamatteh Z. S. H., Raza M., Ahmad T. (1994) Geochemistry of early proterozoic mafic and ultramafic rocks of jharol group, rajasthan, northwestern india. *Geological Society of India* 44:141–156.

Ahmad T., Dragusanu C., Tanaka T. (2008) Provenance of proterozoic basal aravalli mafic volcanic rocks from rajasthan, northwestern india: nd isotopes evidence for enriched mantle reservoirs. *Precambrian Research* 162:150–159. https://doi.org/10.1016/j.precamres.2007.07.011

Ahmad T., Tarney J. (1994) Geochemistry and petrogenesis of late archaean aravalli volcanics, basement enclaves and granitoids, rajasthan. *Precambrian Research* 65:1–23. https://doi.org/10.1016/0301-9268(94)90097-3

Bairwa M. K., Pandit M. K. (2021) Mafic volcanics of raialo group in tehla area, alwar sub-basin: first report of pillow lavas from the north delhi fold belt, northwest india. *J. Earth Syst. Sci.* 130:142. https://doi.org/10.1007/s12040-021-01658-3

Banerjee A. K., Singh S. P. (1977) Sedimentary tectonics of bayana sub-basin of northeastern rajasthan. *Journal of the Indian Association of Sedimentologists* 1:74–85.

Bas M. J. Le, Maitre R. Le, Streckeisen A., Zanettin B. (1986) A chemical classification of volcanic rocks based on the total alkali-silica diagram. *Journal of petrology* 27:745–750. https://doi.org/10.1093/petrology/27.3.745

Biju-Sekhar S., Yokoyama K., Pandit M. K., Okudaira T., Yoshida M., Santosh M. (2003) Late paleoproterozoic magmatism in delhi fold belt, nw India and its implication: Evidence from EPMA chemical ages of zircons. *Journal of Asian Earth Sciences* 22:89–207. https://doi.org/10.1016/S1367-9120(02)00188-8

Bose U., Mathur A. K., Sahoo K. C., Bhattacharya S., Krishan Dutt, Kumar A. V., Sarkar S. S., Choudhary S., Choudhary I. (1996) Event stratigraphy and physicochemical characters of B.G.C. and associated supracrustals in the south mewar plains of rajasthan. *Journal of the Geological Society of India* 47:325–338.

Chakrabarti C., Pyne T. K., Gupta P., Basumallick S., Guha D. (2004) A manual of the geology of india. *Spl. Pub.* 77:175–187.

Chaudhary A. K., Gopalan K., Sastry C. A. (1984) Present status of the geochronology of the precambrian rocks of Rajasthan. *Tectonophys* 105:131–140. https://doi.org/10.1016/0040-1951(84)90199-9

Crawford A. R. (1970) The precambrian geochronology of rajasthan and bundelkhand, northern India. *Canadian Journal of Earth Sciences* 7:91–110. https://doi.org/10.1139/e70-007

Dabiri R., Akbari-Mogaddam M., Ghaffari M. (2018-a) Geochemical evolution and petrogenesis of the eocene Kashmar granitoid rocks, NE Iran: implications for fractional crystallization and crustal contamination processes. *Iranian Journal of Earth Sciences* 10 (1): 68–77.

Deb M., Thorpe R. I., Kristic D., Corfu F., Davis D. W. (2001) Zircon u-Pb and galena pb–isotope evidence for an approximate 1.0 gaterrane constituting the western margin of the aravalli-delhi orogenic belt northwestern india. *Precam Res* 108:195–213. https://doi.org/10.1016/S0301-9268(01)00134-6

Dilek Y., Furnes H. (2011) Ophiolite genesis and global tectonics: geochemical and tectonic fingerprinting of ancient oceanic lithosphere. *Geological Society of America Bulletin* 123:387–411. https://doi.org/10.1130/B30446.1

Drury S. A. (1982) Geochemistry of archaean metavolcanic rocks from the holenarsipur and shigegudda volcanosedimentary belts of karnataka, south india. *Precam Res* 19:119–139. https://doi.org/10.1016/0301-9268(82)90055-9

——— (1983) The petrogenesis and setting of archaean metavolcanics from karnataka state, south India. *Geochimica et Cosmochimica Acta* 47:317–329. https://doi.org/10.1016/0016-7037(83)90144-8

D'Souza J., Sheth H., Xu Y., Wegner W., Prabhakar N., Sharma K. K., Koeberl C. (2020) Neoarchaean crustal reworking in the aravalli craton: petrogenesis and tectonometamorphic history of the malola granite, bhilwara area, northwestern india. *Geological Journal* 55:8186–8210. https://doi.org/10.1002/gj.3927

Gupta B. C. (1934) The geology of central mewar. *Memoir Geol. Surv.* 65:107–168.

Gupta S. N., Arora Y. K., Mathur R. K., Iqballuddin P. B., Sahai T. N., Sharma S. B. (1980) Lithostratigraphic map of the aravalli region. *Geological Survey of India*

Gupta S. N., Arora Y. K., Mathur R. K., Iqbaluddin, Prasad B., Sahai T. N., Sharma S. B. (1997) The precambrian geology of the aravalli region, southern rajasthan and northeastern gujarat. *Mem. Geological Survey of India* 123:262.

Gupta S. N., Mathur R. K., Arora Y. K. (1992) Lithostratigraphy of proterozoic rocks of rajasthan – a review. *Rec. Geol. Surv. India.* 115:63–85.

Heron A. M. (1953) Geology of central rajasthan. *Mem. Geological Survey of India* 79:389.

——— (1922) Geology of western jaipur. *Records Geological Survey of India* 54:345–397.

——— (1917) The geology of north-eastern rajputana and adjacent district. *Mem. Geological Survey of India* 45:1–128.

I G. S. (2001) Geology and mineral resources of rajasthan. *Geological Survey of India, Misc. Publ. 2nd edn.* 30:113.

Irvine T. N., Baragar W. R. A. (1971) A guide to the chemical classification of the common volcanic rocks. *Canadian Journal of Earth Sciences* 8:523–548. https://doi.org/10.1139/e71-055

Jensen L. S. (1976) A new cation plot for classifying subalkalic volcanic rocks. *Department of ministry of natural resources,* 1–66.

Kaur P., Chaudhri N., Raczek I., Kröner A., Hofmann A. W. (2007) Geochemistry, zircon ages and whole-rock nd isotopic systematics for palaeoproterozoic a-type granitoids in the northern part of the delhi belt, rajasthan, nw India: implications for late palaeoproterozoic crustal evolution of the aravalli craton. *Geological Magazine* 144:361–378. https://doi.org/10.1017/S0016756806002950

Kaur P., Chaudhri N., Raczek I., Kröner A., Hofmann A. W., Okrusch M. (2011) Zircon ages of late palaeoproterozoic (ca. 1.72-1.70 ga) extension-related granitoids in ne rajasthan, india: regional and tectonic significance. *Gondwana Research* 19:1040–1053. https://doi.org/10.1016/j.gr.2010.09.009

Kaur P., Zeh A., Okrusch M., Chaudhri N., Gerdes A., Brätz H. (2016) Separating regional metamorphic and metasomatic assemblages and events in the northern khetri complex, nw india: evidence from mineralogy, whole-rock geochemistry and u–pb monazite chronology. *Journal of Asian Earth Sciences* 129:117–141. https://doi.org/10.1016/j.jseaes.2016.08.002

Kepezhinskas P., Defant M., Drummond M. S. (1996) Progressive enrichment of island arc mantle by melt-peridotite interaction inferred from kamchatka xenoliths. *Geochimica et Cosmochimica Acta* 60:1217–1229. https://doi.org/10.1016/0016-7037(96)00001-4

Khanna P. P., Saini N. K., Mukherjee P. K., Purohit K. K. (2009) An appraisal of icp-ms technique for determination of rees: long term qc assessment of silicate rock analysis. *Himalayan Geol.* 30:95–99.

Mckenzie N. R., Hughes N. C., Myrow P. M., Banerjee D. M., Deb M., Planavsky N. J. (2013) New age constraints for the proterozoic aravalli–delhi successions of india and their implications. *Precambrian Research* 238:120–128. https://doi.org/10.1016/j.precamres.2013.10.006

Mullen E. D. (1983) A minor element discriminant for basaltic rocks of oceanic environments and its implications for petrogenesis. *Earth and Planetary Science Letters* 62 (1): 53–62. https://doi.org/10.1016/0012-821X(83)90070-5

Natali C., Beccaluva L., Bianchini G., Siena F. (2017) Comparison among ethiopia-yemen, deccan, and karoo continental flood basalts of central gondwana: insights on lithosphere versus asthenosphere contributions in compositionally zoned magmatic provinces. *Spec. Pap. Geol. Soc. Am.* 526:191–215. https://doi.org/10.1130/2017.2526(10)

Nazari M., Arian M. A., Solgi A., Zareisahamieh R., Yazdi A. (2023) Geochemistry and technomagmatic environment of eocene volcanic rocks in the southeastern region of abhar. *Iranian Journal of Earth Sciences* 15 (4): 228–247. https://doi.org/10.30495/ijes.2023.1956689.1746

Niu Y. (2018) Geological understanding of plate tectonics: basic concepts, illustrations, examples and new perspectives. *Global Tectonics and Metallogeny* 10 (1): 23 –46. https://doi.org/10.1127/gtm/2014/0009

Ousta S. H., Ashja-Ardalan A., Yazdi A., Dabiri R., Arian M. A. (2024) Petrogenesis and tectonic implications of miocene dikes in the southeast of bam (se iran): constraints on the development of active continental margin. *Geopersia* 14 (1): 89–111. https://doi.org/10.22059/geope.2023.364334.648729

Pandit M. K., Khatatneh M. K. (2003) Alkali exchange as a possible mechanism for the genesis of low-k granite: evidence from ajitgarh pluton, proterozoic delhi fold belt, nw india. *J. Geol. Soc. India.* 62:696–707.

Pandit M. K., Kumar H., Wang W. (2021) Geochemistry and geochronology of a-type basement granitoids in the northcentral aravalli craton: implications on paleoproterozoic geodynamics of nw indian block. *Geoscience Frontiers* 12:101084. https://doi.org/10.1016/j.gsf.2020.09.013

Pearce J. A. (1982) Statistical analysis of major element patterns in basalts. *Journal of Petrology* 17 (1): 15–43. https://doi.org/10.1093/petrology/17.1.15

Pearce J. A., Ernst R. E., Peate D. W., Rogers C. (2021) Lip printing: using of immobile elements proxies to characterize large igneous provinces in geologic record. *Lithos* 392-393:106068. 10.1016/j.lithos.2021.106068

Pearce J. A., Norry M. J. (1979) Petrogenetic implications of ti, zr, y, and nb variations in volcanic rocks. *Contributions to Mineralogy and Petrology* 69:33–47. https://doi.org/10.1007/BF00375192

Pearce J. A., Peate D. W. (1995) Tectonic implications of the composition of volcanic arc magmas; ann. rev. *Earth Planet. Sci.* 23:251–285. https://doi.org/10.1146/annurev.ea.23.050195.001343

Ramakrishan M., Vaidyanadhan R. (2008) Geology of india. *Geological Society of India* 1:556.

Rastogi S. K., Ghosh S., Das S., Sinha A. K. (2016) Specialized thematic mapping of delhi supergroup rocks in khodariba–tehla–bhighota–dewati area, dausa and alwar district, rajasthan with special emphasis on the mineral potential of the area; unpublished report of fsp 2015–2016. *Geological Survey of India*

Raza M., Azam M. S., Khan M. S. (2001) Geochemistry of mesoproterozoic mafic volcanics of bayana basin, north delhi fold belt: constraints on mantle source conditions and magmatic evolution. *Journal of the Geological Society of India* 57:507–518.

Raza M., Khan M. S., Azam M. S. (2014) Petrogenetic study of mesoproterozoic volcanic rocks of north delhi fold belt, nw indian shield: implications for mantle conditions during proterozoic. *Chinese Journal of Geochemistry* 4:93–114. https://doi.org/10.1007/s11631-014-0024-4

——— (2007) Plate-plume accretion tectonics in proterozoic terrain of northeastern rajasthan, india: evidence from mafic volcanic rocks of north delhi fold belt. *Island Arc* 16:536–552. https://doi.org/10.1111/j.1440-1738.2007.00581.x

Rollinson H. R. (1993) Using geochemical data: evaluation, presentation,interpretation. *Longman Essex*

Roy A., Paliwal B. S. (1981) Evolution of lower proterozoic epicontinental deposits stromatolite bearing aravalli rocks of udaipur, rajasthan, india. *Precambrian Research* 14:49–74. https://doi.org/10.1016/0301-9268(81)90035-8

Roy A. B., Jakhar S. R. (2002) Geology of rajasthan (northwestern india) precambrian to recent. *Scientific Publishers (India),* 421.

Roy A. B., Kataria P. (1999) Precambrian geology of the aravalli mountain and neighbourhood: analytical update of recent studies. *Proc. Sem. Geology of Rajasthan: Status and Perspective, MLS University,* 1–56.

Saini N. K., Mukherjee P. K., Khanna P. P., Purohit K. K. (2007) A proposed amphibolite reference rock sample (amh) from himachal pradesh. *Journal of the Geological Society of India* 69:799–802.

Sing S. P. (1988) Sedimentation patterns of the proterozoic delhi supergroup, northern rajasthan, india, and their tectonic implications. *Sedimentary Geology* 58:79–94. https://doi.org/10.1016/0037-0738(88)90007-3

Singh K. S., Waele B. D., Karmakar S., Sarkar S., Biswal T. K. (2010) Tectonic setting of the balaram–kui–surpagla–kengora granulites of the south delhi terrane of the aravalli mobile belt, nw india and its implication on correlation with the east african orogen in the gondwana assembly. *Precambrian Research* 183 (4): 669–688. https://doi.org/10.1016/j.precamres.2010.08.005

Singh S. P. (1984) Evolution of the proterozoic alwar sub basin, northeastern rajasthan. *Indian Journal of Earth Science, CEISM, Seminar Volume,* 113–124.

Sinha-Roy S. (1984) Precambrian folded unconformity in rajasthan. *Current Science* 53:1205–1207.

Sinha-Roy S., Malhotra G., Mohanty M. K. (1998) The geology of rajasthan. *Geological Society of India* 278

Subbarao K. V., Hooper R. R. (1988) Reconnaissance map of the deccan basalt group in the western ghats, india scale 1: 100000 in: deccan flood basalts. *Mem. Geological Society of India* 10

Sun S. S., McDonough W. F. (1989) Chemical and isotopic systematics of oceanic basalts: implications for mantle composition and processes, geological society, london. *Special Publications* 42:313–345. https://doi.org/10.1144/GSL.SP.1989.042.01.19

Verma S. P., Agrawal S. (2011) New tectonic discrimination diagrams for basic and ultrabasic volcanic rocks through log-transformed ratios of high field strength elements and implications for petrogenetic processes. *Revista Mexicana de Ciencias Geológicas* 28:24–44.

Wall H. de, Pandit M. K., Donhauser I., Schobel S., Wang W., Sharma K. K. (2018) Evolution and tectonic setting of the malani–nagarparkar igneous suite: a neoproterozoic silicic-dominated large igneous province in nw india–SE pakistan. *Journal of Asian Earth Sciences* 160:136–151. https://doi.org/10.1016/j.jseaes.2018.04.016

Wang W., Cawood P. A., Pandit M. K., Zhou M. F., Chen T. C. (2017) Zircon u–Pb age and hf isotope evidence for an eoarchean crustal remnant and episodic crustal reworking in response to supercontinent cycles in nw india. *Journal of the Geological Society* 174 (4): 759–772. https://doi.org/10.1144/jgs2016-080

Wiedenbeck M., Goswami J. N., Roy A. B. (1996) Stabilization of the aravalli craton of northwestern india at 2.5 ga: an ion microprobe zircon study. *Chem. Geol.* 129:325–340. https://doi.org/10.1016/0009-2541(95)00182-4

Wilson M. (1989) Igneous petrogenesis: a global tectonic approach. *Unwin Hyman, London* 466 https://doi.org/10.1007/978-94-010-9388-0

Winchester J., Floyd P. (1977) Geochemical discrimination of different magma series and their differentiation products using immobile elements. *Chemical geology* 20:325–343. https://doi.org/10.1016/0009-2541(77)90057-2